Strange hadron production at low transverse momenta

Gábor I Veres

Laboratory for Nuclear Science, Massachusetts Institute of Technology, Bldg. 24-422, 77 Massachusetts Avenue, Cambridge, MA 02139-4307, USA

E-mail: veres@mit.edu

for the PHOBOS Collaboration:

B.B.Back[1], M.D.Baker[2], M.Ballintijn[4], D.S.Barton[2], B.Becker[2], R.R.Betts[6], A.A.Bickley[7], R.Bindel[7], A.Budzanowski[3], W.Busza[4], A.Carroll[2], M.P.Decowski[4], E.García[6], T.Gburek[3], N.George[1,2], K.Gulbrandsen[4], S.Gushue[2], C.Halliwell[6], J.Hamblen[8], A.S.Harrington[8], C.Henderson[4], D.J.Hofman[6], R.S.Hollis[6], R.Hołyński[3], B.Holzman[2], A.Iordanova[6], E.Johnson[8], J.L.Kane[4], N.Khan[8], P.Kulinich[4], C.M.Kuo[5], J.W.Lee[4], W.T.Lin[5], S.Manly[8], A.C.Mignerey[7], A.Noell[7], R.Nouicer[2,6], A.Olszewski[3], R.Pak[2], I.C.Park[8], H.Pernegger[4], C.Reed[4], L.P.Remsberg[2], C.Roland[4], G.Roland[4], J.Sagerer[6], P.Sarin[4], P.Sawicki[3], I.Sedykh[2], W.Skulski[8], C.E.Smith[6], P.Steinberg[2], G.S.F.Stephans[4], A.Sukhanov[2], R.Teng[8], M.B.Tonjes[7], A.Trzupek[3], C.Vale[4], G.J. van Nieuwenhuizen[4], R.Verdier[4], G.I.Veres[4], B.Wadsworth[4], F.L.H.Wolfs[8], B.Wosiek[3], K.Woźniak[3], A.H.Wuosmaa[1], B.Wysłouch[4], J.Zhang[4]

[1] Argonne National Laboratory, Argonne, IL 60439-4843, USA

[2] Brookhaven National Laboratory, Upton, NY 11973-5000, USA

[3] Institute of Nuclear Physics, Kraków, Poland

[4] Massachusetts Institute of Technology, Cambridge, MA 02139-4307, USA

[5] National Central University, Chung-Li, Taiwan

[6] University of Illinois at Chicago, Chicago, IL 60607-7059, USA

[7] University of Maryland, College Park, MD 20742, USA

[8] University of Rochester, Rochester, NY 14627, USA

Abstract. Some of the latest results of the PHOBOS experiment from the $\sqrt{s_{NN}}$=200 GeV Au+Au data are discussed. Those relevant to strangeness production are emphasized. These observations relate to the nature of the matter created when heavy ions collide at the highest achieved energy.

The invariant yields of strange and non-strange charged hadrons at very low transverse momentum have been measured, and used to differentiate between different dynamical scenarios.

In the intermediate transverse momentum range, the measured ratios of strange and anti-strange kaons approach one, while the antibaryon to baryon ratio is still significantly less, independent of collision centrality and transverse momentum. At high transverse momenta, we find that central and peripheral Au+Au collisions produce similar numbers of charged hadrons per participant nucleon pair, rather than per binary nucleon-nucleon collision.

Finally, we describe the upgrades of PHOBOS completed for the 2003 d+Au and p+p run, which extend the transverse momentum range over which particle identification is possible, and, at the same time, implement a trigger system selective for high-p_T particles.

PACS numbers: 25.75.-q, 13.85.Ni, 21.65.+f

Submitted to: *J. Phys. G: Nucl. Part. Phys.*

1. Introduction

The Relativistic Heavy Ion Collider (RHIC) has continued to provide heavy-ion beams of energies up to 100 GeV per nucleon, which is the highest ever reached in laboratory experiments. PHOBOS, together with the other three RHIC experiments, continues to write a new chapter in the study of nuclear matter under extreme compression and energy density, which RHIC opened in Summer 2000. In this new regime, the created system is dominated by newly produced quarks and gluons, and it exhibits a smaller net baryon density than at lower energies. The substantial number of produced strange and heavier quarks are important probes used to study the differences between purely hadronic phenomena and the collective behaviour of the hot and dense quark-gluon matter expected to be produced in these collisions.

In the 2003 data taking period, deuteron and gold beams were used to obtain a reference dataset to clarify various features of the data from the Au+Au run. This was followed by collisions of polarized proton beams, which are currently being recorded and analysed. In this talk we focus on the results obtained from the Au+Au reactions.

PHOBOS is one of the two small-scale experiments at RHIC, with a technology based on highly segmented silicon sensors. Important parts of the silicon detector are the cylindrical multiplicity array and the three ring-shaped modules on both sides of the interaction point. These give a total pseudo-rapidity coverage of $-5.4 < \eta < +5.4$, which is the largest coverage of the four RHIC experiments.

The two-arm spectrometer is placed in a 2.1 Tesla magnetic field, in which particle trajectories from about 10 MeV/c to about 10 GeV/c momentum can be measured. Particle identification is provided by the specific energy loss as well as by scintillator time-of-flight (ToF) detectors. The trigger system can be changed from a minimum bias to a selective high-p_T trigger, at the same time delivering various on-line and off-line measures of vertex position and collision centrality both in Au+Au and d+Au collisions. In 2003, the experiment was upgraded by adding new start-time detectors, which are used to generate a start signal for the ToF measurements and to provide on-line vertex information for the trigger system, lead-scintillator calorimeter arrays in both very forward directions, and a scintillator array providing a high-p_T trigger by means of simple on-line tracking. Details of the setup and the layout of the subdetectors can be found elsewhere [1].

The PHOBOS detector system has different particle identification capabilities for various transverse momentum ranges:

- p_T < 200 MeV/c: mass identification,
- 0.2 GeV/c < p_T < 1 GeV/c: mass and charge identification based on dE/dx and momentum measurements;
- 0.2 GeV/c < p_T < 2-4 GeV/c (setup dependent): mass and charge identification based on time-of-flight and momentum measurements;
- 2-4 GeV/c < p_T: charge identification only.

It is therefore natural to divide the talk into the four following sections, dealing with the above regimes.

2. Identified hadrons in the low p_T range

The measurement of identified particle yields at very low transverse momenta was one of the original PHOBOS design goals. The particle yields at low p_T can be compared with predictions of various models like the collective radial expansion in the framework of hydrodynamical models [2], saturation models addressing the flattening of the p_T spectra at low p_T [3].

In PHOBOS, the Be beam pipe and the proximity (<10 cm) of the first Si layers to the interaction point uniquely permits the measurement and identification of very low-momentum particles. The charge sign of the particles cannot be measured in this momentum range due to the lack of magnetic field, and thus we present invariant yields of $(\pi^+ + \pi^-)$, $(K^+ + K^-)$ and $(p + \overline{p})$.

The measurement was carried out in the 2001 Au+Au run; the triggering and event centrality selection were based on a pair of scintillator counter rings, covering $3 < |\eta| < 4.5$ [1]. For this analysis, 15% of the most central Au+Au collisions were selected (0.4 million events) with reconstructed vertex positions between -7 and $+15$ cm along the beam axis (0 is defined by the nominal interaction point of the beams).

Particles ranging out in the fifth Si layer were selected. To reconstruct the particle trajectories and mass, we studied the energy deposition in the first sensor layers. Strict cuts were applied, derived from the analysis of stopping particles obtained from a GEANT simulation of the PHOBOS detector.

For each straight track candidate the total energy deposited, $E_{tot} = \Sigma_{i=1}^{5} dE^i$, was calculated. At low momenta, the specific energy loss is proportional to $1/\beta^2$ in any layer, and the total energy loss after a given layer is approximately the (non-relativistic) kinetic energy (proportional to β^2). The mass parameter M_p^i defined for each layer ($i = 1, ..., 5$) as $M_p^i = (dE/dx)^i \Sigma_{j=i}^{5} dE^j$ will be proportional to the mass m: $M_p \propto m\beta^2/\beta^2 = m$.

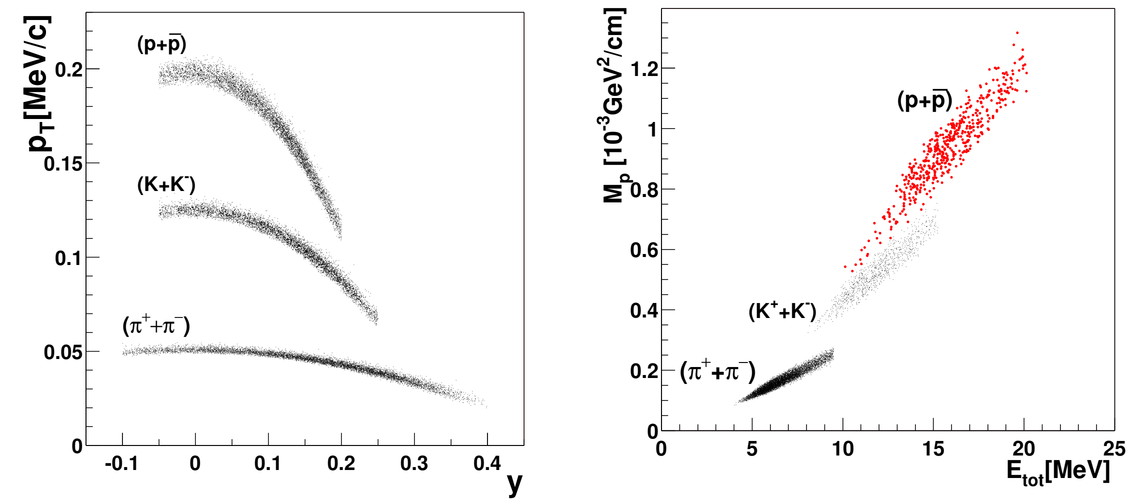

Figure 1. In the left panel, the acceptance for single reconstructed low-p_T particles is shown in the Monte Carlo simulation. For a given rapidity, the p_T is fixed by the requirement that the reconstructed particles should stop in the fifth Si layer. In the right panel, reconstructed particles in the Au+Au data after the cuts are visible; the three islands correspond to the different particle species.

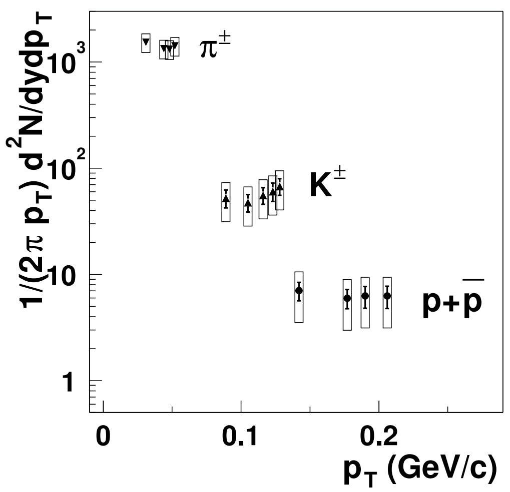

Figure 2. Preliminary invariant yields as a function of p_T. The boxes show systematic errors.

To accept a track candidate, the mass parameter values for the various layers were required to be consistent.

Detailed Monte Carlo studies show that the requirement of stopping the particle in the fifth layer is a strong constraint. It restricts the specific energy loss to certain values which depend, to a good approximation, on the mass only. Thus, by making cuts on these dE/dx values, we can select different particle types. Similarly, the momenta of stopping particles are restricted to a 5% range, the position of which depends only on the mass and the amount of material traversed. The latter varies with the emission angle (and hence the rapidity). The left panel of figure 1 shows the acceptance in transverse momentum and rapidity for the various species. In the right panel, the mass parameter and the total energy loss for stopping particles is plotted for the Au+Au data, after the cuts have been applied.

The data were divided into p_T bins: the corrections for geometrical acceptance, track reconstruction efficiency, particle identification inefficiencies, and for absorption in the beampipe were applied separately. Finally, the contamination due to weak decay products, secondary particles, misidentified and 'ghost' tracks was subtracted. Our estimates of the systematic uncertainties are ±20% for pions, ±40% for kaons and ±50% for protons and include systematic effects in the measured yields and in the estimated correction factors. Figure 2 shows (preliminary) results for invariant yields of $(\pi^+ + \pi^-)$, $(K^+ + K^-)$ and $(p + \overline{p})$ measured at mid-rapidity in the transverse momentum ranges of 30-50 MeV/c for pions, 90-130 MeV/c for kaons and 140-210 MeV/c for protons and antiprotons for the 15% most central Au+Au collisions at $\sqrt{s_{NN}} = 200$ GeV.

It was shown [4] that the RQMD [5] and HIJING [6] models, and a single freeze-out thermal model [2] have difficulty in describing the π, K and p yields at the same time. The yield of $(p + \overline{p})$ bears the most selective power between the models. We conclude that the flattening of the proton spectra attributed to collective radial expansion extends down to very low p_T. Our data agree with extrapolations of measurements performed in the intermediate p_T range [7] and are well described by hydrodynamical calculations [8]. Thus we see no enhancement in particle yields at very low transverse momenta which could be attributed to new long-wavelength physics phenomena.

3. Antiparticle to particle ratios in the medium p_T range

In Au+Au collisions at $\sqrt{s_{NN}}$=200 GeV the baryon density at midrapidity is dominated by baryon production, not baryon transport. The net baryon-free regime thus approached is more appropriate for comparison with first-principle QCD calculations. The study of the energy dependence of particle ratios between $\sqrt{s_{NN}}$ =130 GeV and $\sqrt{s_{NN}}$ =200 GeV thus allows tests of models of baryon production and transport.

In the 0.07-1 GeV/c momentum range, our Si spectrometer provides particle identification via momentum and dE/dx measurements. Ratios between particle and antiparticle yields have been evaluated inclusively as well as a function of collision centrality and transverse momentum.

The rapidity range of the measurement is 0.2-0.8 for protons and kaons, and 0.35-1.3 for pions. The 12% most central Au+Au events taken in the 2001 run were used for evaluating the inclusive ratio, with the estimated mean number of participants being $\langle N_{part}\rangle = 317 \pm 10$ (syst).

Only events with a vertex position between -6 and +6 cm along the beamline were used, thus suppressing

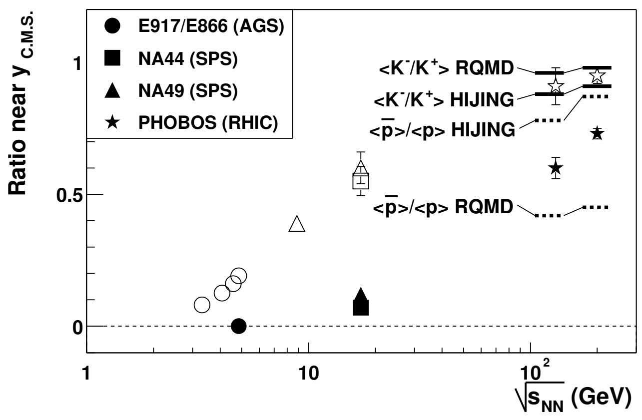

Figure 3. $\langle K^- \rangle / \langle K^+ \rangle$ (open symbols) and $\langle \overline{p} \rangle / \langle p \rangle$ (closed symbols) as a function of $\sqrt{s_{NN}}$ for A+A collisions, compared to HIJING and RQMD. The 12% most central events were used for PHOBOS, 5% for NA49, 6% for NA44, 5% for AGS $\langle K^- \rangle / \langle K^+ \rangle$, and 8% for AGS $\langle \overline{p} \rangle / \langle p \rangle$. Only statistical errors are shown.

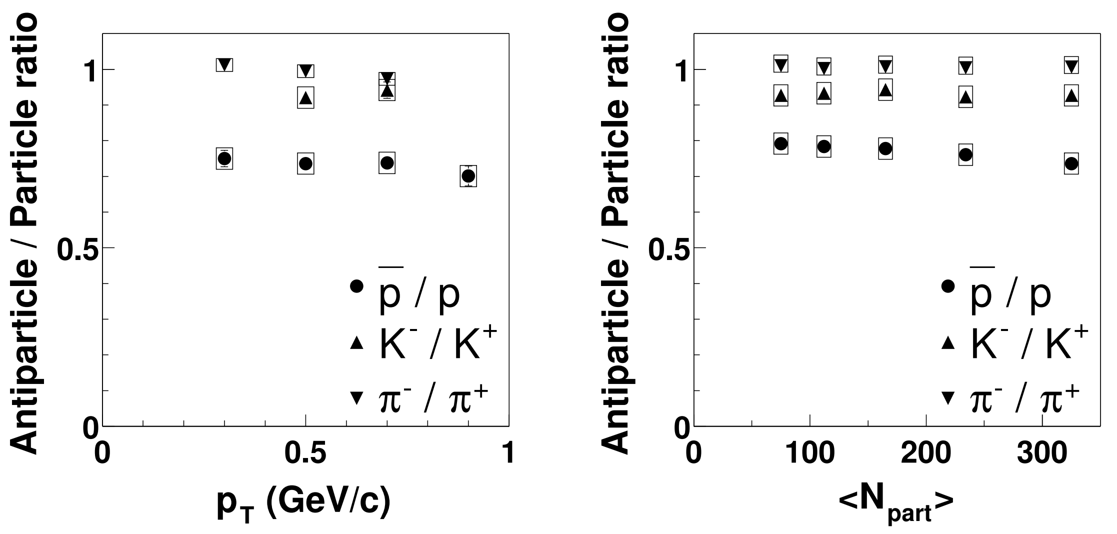

Figure 4. Preliminary antiparticle to particle ratios as a function of transverse momentum for selected central Au+Au collisions (left panel); and as a function of collision centrality (right panel). Boxes represent systematic errors.

the vertex position dependence of the spectrometer acceptance. The ratio determination relies on the cancellation of acceptance, efficiency and background effects between the two magnet polarity settings, which was carefully verified in [9]. Systematic errors due to these effects were estimated to be less than 2%. Contamination by misidentified particles affected the ratios by 0.1-0.8%, depending on particle species. In the case of the pion and the kaon ratios, we applied a correction of less than 1% for secondary particles, absorption in the beampipe and detector material, and daughters of weakly decaying hadrons. These corrections were 1.2% in the case of the $\overline{p}/p$ ratio. The results [9] are (with conservatively assigned systematic errors):

$$\langle\pi^-\rangle\,/\,\langle\pi^+\rangle = 1.025 \pm 0.006\ \text{(stat)}\ \pm 0.018\ \text{(syst)}$$
$$\langle K^-\rangle\,/\,\langle K^+\rangle = 0.95 \pm 0.03\ \text{(stat)}\ \pm 0.03\ \text{(syst)}$$
$$\langle\overline{p}\rangle\,/\,\langle p\rangle = 0.73 \pm 0.02\ \text{(stat)}\ \pm 0.03\ \text{(syst)}.$$

The measured proton ratios, shown in figure 3, follow the trends observed at lower energies, but are in significant disagreement with HIJING [6] and RQMD [5] predictions, constraining current and future models dealing with baryon production and transport. Using a statistical model calculation [10], we estimate $\mu_B/T = 0.17 \pm 0.01$ (stat), where μ_B is the chemical potential and T is the freeze-out temperature. Taking a typical freeze-out temperature of 165 MeV, we obtain $\mu_B = 27 \pm 2$ (stat) MeV, which is about half of the 130 GeV value of $\mu_B = 45 \pm 5$ (stat) MeV [11].

The left panel of figure 4 shows preliminary results for the dependence of antiparticle to particle ratios on transverse momentum for the 10% most central Au+Au collisions at $\sqrt{s_{NN}} = 200$ GeV. Within our uncertainties, the ratios are independent of p_T in the measured rapidity and p_T range. The centrality dependence of the measured ratios is

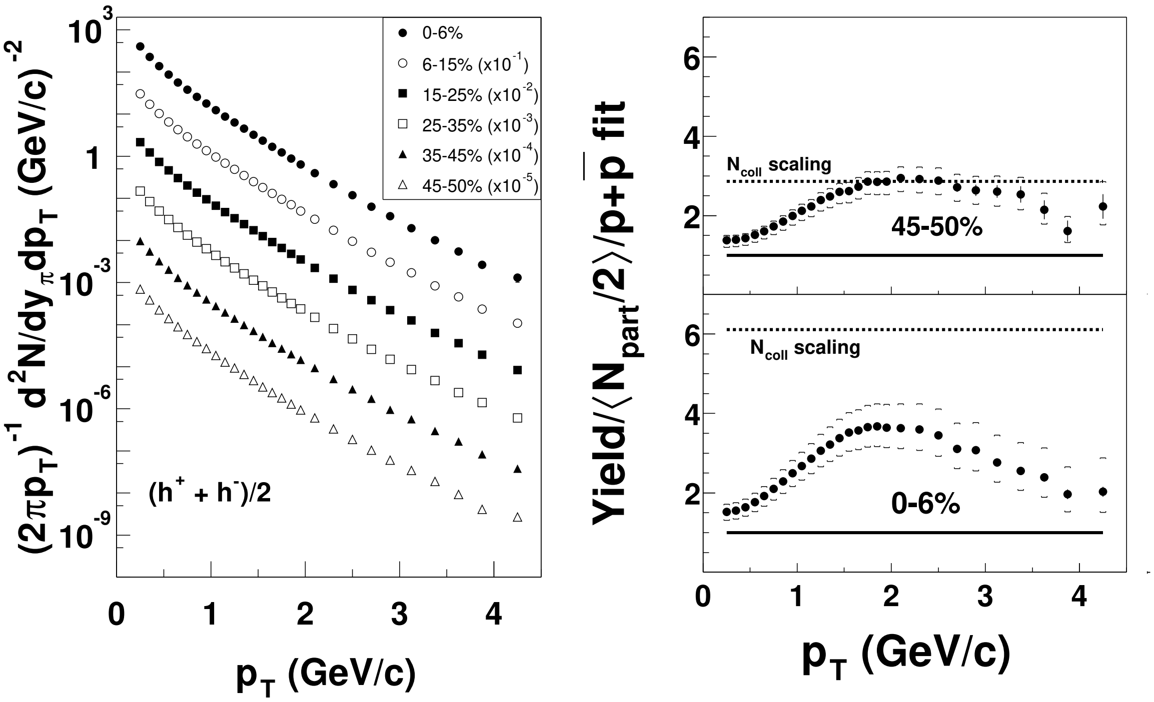

Figure 5. Left panel: Invariant yields for charged hadrons as a function of p_T for six centrality bins. Consecutive bins were scaled by factor of 10. Statistical and systematic errors are smaller than the symbol size. Right panel: ratio of the yield of charged hadrons as a function of p_T for the most peripheral ($\langle N_{part}\rangle = 65 \pm 4$) and the most central ($\langle N_{part}\rangle = 344 \pm 11$) bin to a fit of proton-antiproton data, scaled by $\langle N_{part}\rangle /2$. The dashed (solid) line shows the expectation of N_{coll} (N_{part}) scaling relative to $p+\overline{p}$ collisions. The brackets show the systematic uncertainty of the Au+Au data.

shown in the right panel. The pion and kaon ratios are consistent with a constant value over the measured centrality range. For the $\langle\overline{p}\rangle / \langle p\rangle$ ratio, a weak but systematic drop with N_{part} can be observed, although, within our systematic errors, the ratio is also consistent with constant.

4. Particle spectra at high transverse momenta

In this section we present transverse momentum distributions of charged hadrons produced in Au+Au collisions at $\sqrt{s_{NN}} = 200$ GeV, measured between 0.25< p_T <4.5 GeV/c in the rapidity range of 0.2< y_π <1.4. The evolution of the spectra is studied as a function of collision centrality, from 65 to 344 participating nucleons.

Figure 5 shows the measured p_T spectra, corrected for the geometrical acceptance of the detector, the efficiency of the tracking algorithm, and distortion due to finite momentum resolution and variable bin widths, secondary and feed-down contributions from weak decays, and wrongly reconstructed 'ghost' tracks. The yields were averaged over positive and negative charge signs.

In the right panel of figure 5, the results are compared to data from $p+\overline{p}$ collisions where the Au+Au data for the most peripheral ($\langle N_{part}\rangle = 65 \pm 4$) and the most central ($\langle N_{part}\rangle = 344 \pm 11$) bin were divided by a fit of the measured p_T distribution in proton-antiproton collisions at the same energy [12]. We find a significant change of spectral shape already between $p+\overline{p}$ and semi-peripheral Au+Au collisions.

So-called 'hard' processes are expected to dominate particle production at high transverse momenta. Hard processes are expected to scale with the number of binary nucleon-nucleon collisions N_{coll}, whereas 'soft' particle production is expected to scale with the number of participating nucleons N_{part}. The collision centrality, and therefore the N_{coll}/N_{part} ratio, can be varied experimentally. Thus, we expect a change in the relative contributions of hard and soft processes as well.

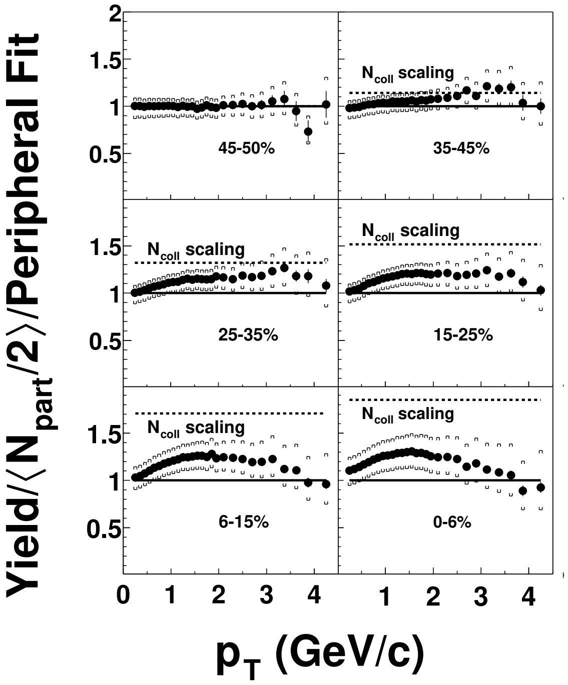

Figure 6. Charged hadron yields in Au+Au collisions in six centrality bins, divided by a fit to the most peripheral bin and by $N_{part}/N_{part}^{periph.}$. The dashed (solid) line shows the expectation of N_{coll} (N_{part}) scaling relative to peripheral collisions. The brackets show systematic uncertainties of the Au+Au data.

Comparing peripheral to central Au+Au collisions, we find that the yields at high p_T exhibit approximate scaling with N_{part}, rather than with N_{coll}. This is further illustrated in figure 6 where the spectra are divided by a fit to the most peripheral bin and by the ratio between the N_{part} of the bin shown and the N_{part} of the peripheral bin. N_{part} scaling would correspond to the ratio being constant at unity (solid line), whereas N_{coll} scaling, shown by the dashed line, would lead to an increase by a factor of two from peripheral to central events. We observe that in the low and high transverse momentum regions approximate N_{part} scaling applies, whereas in the 1.5-3 GeV/c range there is an excess above N_{part} scaling and a deficiency below N_{coll} scaling [13].

This suppression of the particle yields at intermediate and high p_T was observed earlier in Au+Au collisions at $\sqrt{s_{NN}}$ =130 GeV, where it was interpreted as the result of particle energy loss in a dense medium. The observed approximate scaling with N_{part} is a result of an interplay between initial and final state effects [14]. It has recently been argued that the observed scaling could be explained by invoking surface emission of high-p_T hadrons [15], or in the context of initial state saturation models [16]. The already published new experimental results on d+Au collisions [17] provide further insight into the modification of particle spectra in a nuclear environment.

5. Identification and triggering capabilities in d+Au and p+p collisions

Finally, we briefly discuss the PHOBOS detector upgrades relevant for identified high-p_T spectra, completed in December 2002 in preparation for the ongoing d+Au and p+p run at RHIC.

Among other important upgrades, a new set of start-time Cerenkov counters have been installed on both sides of the interaction point for better efficiency and precision of the ToF measurement. The ToF scintillator walls have been moved about 2.5 times further away from the interaction point to increase the accessible p_T range for particle identification. This has decreased the geometrical acceptance of the walls. To enhance the number of events where a high-p_T particle hits the ToF walls even at low track multiplicity, the ToF walls have been incorporated in the higher level trigger of PHOBOS.

In addition, a new pair of segmented scintillator hodoscopes (spectrometer trigger) have been installed between the ToF walls and the interaction point. The new start-time detectors provided an approximate vertex position, which, together with the hit positions in the spectrometer trigger and the ToF walls, allowed for a simple on-line tracking that selects straight line (high-p_T) trajectories. Technically, the necessary logic equations were implemented in a field programmable gate array, which provides a trigger decision in less than 50 ns. Figure 7 illustrates the principle of operation for the detectors located at a 45° angle with respect to the beamline. There is another pair of similar walls at 90° in order to maximize the coverage in p_T and in rapidity. The silicon layers of the magnetic spectrometer arms, one of the spectrometer trigger walls, and one of the ToF walls (at a 45° angle) are shown in figure 7.

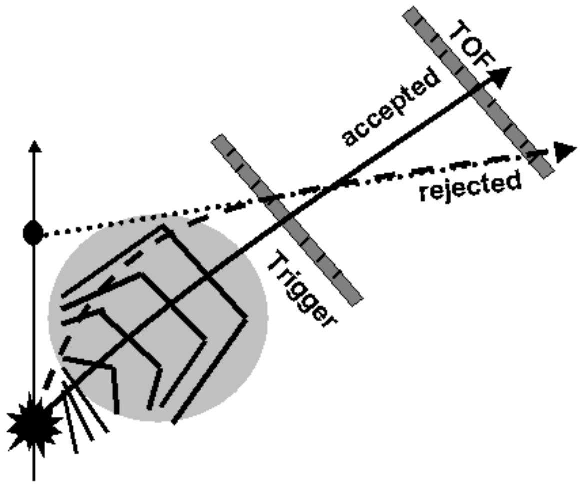

Figure 7. Schematic of the high-p_T selective spectrometer trigger operated in the 2003 d+Au and p+p run.

The new trigger was used successfully in the 2003 RHIC run. Our data sample of high-p_T tracks in the ToF walls was enhanced by a factor of 15, with respect to the simple minimum bias trigger. As a first step in the data analysis, charged hadron spectra using data from the new setup have been already published [17].

Figure 8 shows a comparison of transverse momentum spectra using the minimum bias trigger (left panel) and the new spectrometer trigger (right panel). The figures show all the tracks collected in the Si spectrometer arms (solid line). Separate histograms indicate the yield of tracks with a ToF hit (dashed line), the tracks detected by both the ToF and the spectrometer trigger walls (diagonal lines), and finally the tracks which

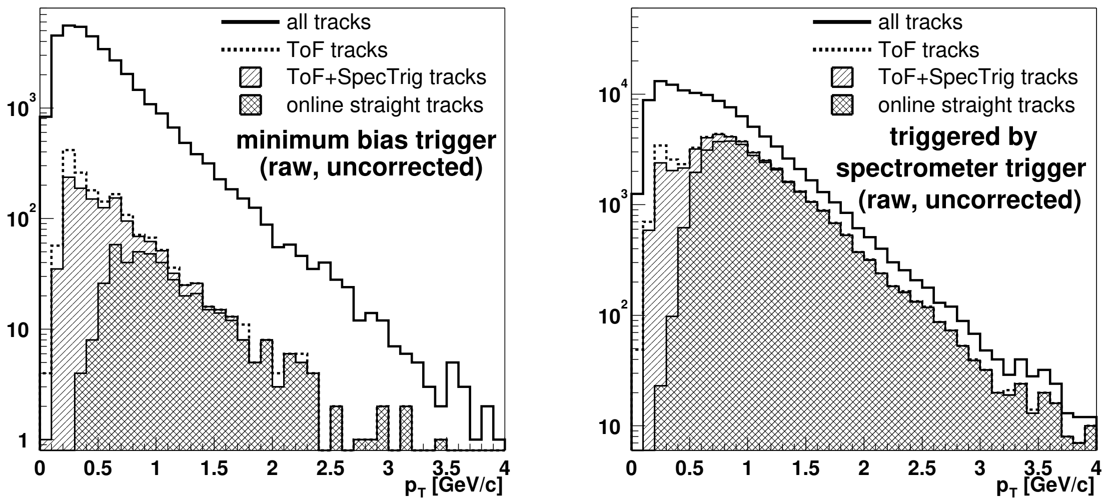

Figure 8. Uncorrected raw p_T distributions with the minimum bias trigger (left panel) and the new spectrometer trigger (right panel).

also satisfy the logic equations requiring that the on-line vertex point and the two hit positions in the scintillator counters are approximately on a straight line (hatched). This selection suppresses the low-p_T part of the particle spectrum, and the detector approaches 95% efficiency only between 1.5 and 2 GeV/c. The fraction of high-p_T particles with a ToF hit has thus dramatically increased.

These upgrades increase the potential of the PHOBOS apparatus to analyze identified particle ratios and spectra in the p_T range starting from 1 GeV/c, where the specific energy loss in the Si spectrometer no longer differs significantly between particle species, and hurts the particle identification. In the 2.5-4.5 GeV/c transverse momentum range, the suppression of charged particle yields with respect to the expected N_{coll} scaling (presented in Section 4) is of central interest. With the new data, comparison between identified particle spectra in Au+Au and d+Au collisions will become possible.

6. Summary

At the very low p_T range we have presented unique measurements of invariant yields of identified particles, showing no evidence of enhancement of the yields, and indicating the important role of radial expansion. In the $p_T < 1$ GeV/c range we found antiparticle-particle ratios independent of collision centrality and p_T within our systematic uncertainties. The antiproton to proton ratio suggests a baryochemical potential two times smaller at $\sqrt{s_{NN}}$ =200 GeV than at $\sqrt{s_{NN}}$ =130 GeV. At higher p_T (up to 4.5 GeV/c) we have found that the charged hadron spectra scale approximately with the number of participating nucleons rather than with the number of binary nucleon-nucleon collisions. We have presented details of the upgrade of the PHOBOS setup relevant to the particle identification, and a new high-p_T selective trigger operated during the 2003 d+Au and p+p runs at RHIC.

Acknowledgments

We acknowledge the generous support of the Collider-Accelerator Department (including RHIC project personnel) and Chemistry Department at BNL. This work was partially supported by U.S. DOE grants DE-AC02-98CH10886, DE-FG02-93ER40802, DE-FC02-94ER40818, DE-FG02-94ER40865, DE-FG02-99ER41099, and W-31-109-ENG-38 as well as NSF grants 9603486, 9722606 and 0072204. The Polish group was partially supported by KBN grant 2-P03B-10323. The NCU group was partially supported by NSC of Taiwan under contract NSC 89-2112-M-008-024.

References

[1] Back B B *et al* 2003 *Nucl. Instrum. Methods* **A 499** 603-623
[2] Broniowski W, Florkowski W 2001 *Phys. Rev. Lett.* **87** 272302
[3] Schaffner-Bielich J *et al* 2002 *Preprint* nucl-th/0202054
[4] Wosiek B *et al* 2003 *Nucl. Phys.* **A 715** 510
[5] Sorge H 1991 *Phys. Rev.* **C 52** 3291
[6] Gyulassy M, Wang X N 1993 *Comput. Phys. Commun* **83** 307
[7] Ullrich T S 2003 *Nucl. Phys.* **A 715** 399
[8] Kolb P F, Rapp R 2003 *Phys. Rev.* **C 67** 044903
[9] Back B B *et al* 2003 *Phys. Rev.* **C 67** 021901R
[10] Becattini F *et al* 2001 *Phys. Rev.* **C 64** 024901
[11] Back B B 2001 *Phys. Rev. Lett.* **87** 102301
[12] Albajar C *et al* 1990 *Nucl. Phys.* **B 335** 261
[13] Back B B *et al* 2003 *Preprint* nucl-ex/0302015
[14] Adcox K *et al* 2002 *Phys. Rev. Lett.* **88** 022301
[15] Müller B 2003 *Phys. Rev.* **C 67** 061901
[16] Kharzeev D *et al* 2003 *Phys. Lett.* **B 561** 93
[17] Back B B *et al* 2003 *Phys. Rev. Lett.* **91** 072302